

# Thermal decomposition of $\text{CuCrO}_4 \cdot 2\text{CuO} \cdot 2\text{H}_2\text{O}$ and phase relations in the Cu–Cr–O system

G. M. KALE

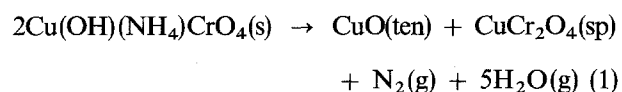
*Department of Mining and Mineral Engineering, University of Leeds, Leeds, LS2 9JT, UK*

The compound,  $\text{CuCrO}_4 \cdot 2\text{CuO} \cdot 2\text{H}_2\text{O}$  has been synthesized by precipitating it from the aqueous solution containing chromium (VI) oxide and basic copper (II) carbonate. Thermal decomposition of  $\text{CuCrO}_4 \cdot 2\text{CuO} \cdot 2\text{H}_2\text{O}$  has been studied by thermogravimetry and differential scanning calorimetry in flowing air and pure oxygen between 298 and 1373 K. The formation of different phases after each stage of decomposition were identified by X-ray diffraction analysis. The compound  $\text{CuCrO}_4$  was found to be non-stoichiometric. Based on the results obtained in this study and those reported earlier, the isothermal section of the phase diagram of the Cu–Cr–O ternary system has been composed at 600 and 1150 K. Scanning electron microscopy studies of  $\text{CuCrO}_4 \cdot 2\text{CuO} \cdot 2\text{H}_2\text{O}$  precipitate showed rectangular plate-like morphology. The decomposition of  $\text{CuCrO}_4 \cdot 2\text{CuO} \cdot 2\text{H}_2\text{O}$  at 798 K in air resulted in the formation of a mixture of fine powder of  $\text{CuCr}_2\text{O}_4 + \text{CuO}$  (Adkin's catalyst) having a uniform spherical geometry and a particle size less than 0.1  $\mu\text{m}$ .

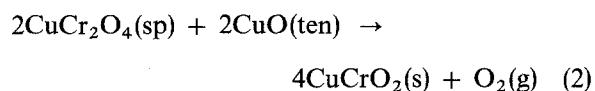
## 1. Introduction

The catalytic activity and selectivity of ternary oxides in the Cu–Cr–O system is well known for several oxidation, hydrogenation, dehydrogenation and alkylation processes. The Adkin's catalyst [1–3] which is constituted of CuO and  $\text{CuCr}_2\text{O}_4$  phases, forms a part of the ternary Cu–Cr–O system. The catalytic activity of Adkin's catalyst generally depends on the method of preparation and the pretreatment [4]. The catalytic activity is significantly influenced by the crystallite size of phases, oxidation state of metal ions, distribution of cations on crystallographically non-equivalent, tetrahedral and octahedral, sites of  $\text{CuCr}_2\text{O}_4$  with a 2–3 spinel structure and the non-stoichiometry of the phases.

Synthesis of Adkin's catalyst by the autocatalytic thermal decomposition of  $\text{Cu}(\text{OH})(\text{NH}_4)\text{CrO}_4$  complex takes place according to the reaction [1, 5]

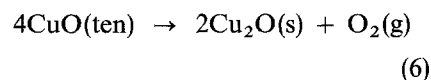
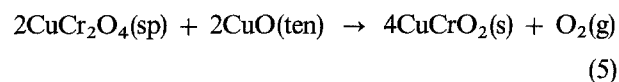
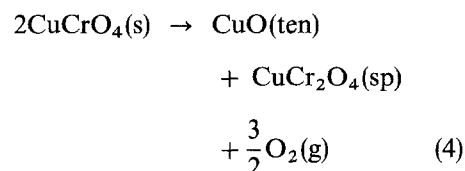
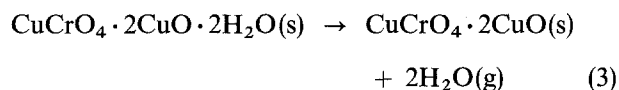


At higher temperature and reduced oxygen partial pressure,  $\text{Cu}^{2+}$  reduces to  $\text{Cu}^+$  in the spinel phase according to the reaction [6]



The Adkin's catalyst can be synthesized by thermal dissociation of coprecipitated copper and chromium hydroxides or hydroxynitrates [7, 8], copper chromate ( $\text{CuCrO}_4$ ) precipitated from the aqueous solution of cupric nitrate and ammonium dichromate [9] or by direct solid-state reaction between CuO and

$\text{Cr}_2\text{O}_3$  at elevated temperature. There is no report in the literature of synthesis of Adkin's catalyst by thermal dissociation of  $\text{CuCrO}_4 \cdot 2\text{CuO} \cdot 2\text{H}_2\text{O}$  precipitated from the aqueous solution of chromium (VI) oxide and basic copper(II) carbonate. Therefore, in this paper, the results of an investigation of the thermal decomposition of  $\text{CuCrO}_4 \cdot 2\text{CuO} \cdot 2\text{H}_2\text{O}$  are reported. The process of decomposition of  $\text{CuCrO}_4 \cdot 2\text{CuO} \cdot 2\text{H}_2\text{O}$  was monitored by thermogravimetry (TG) and differential scanning calorimetry (DSC) between 298 and 1373 K in a dynamic atmosphere of pure oxygen and air. The formation of different phases after each stage of decomposition was identified by X-ray diffraction (XRD). The decomposition temperatures for solid  $\text{CuCrO}_4 \cdot 2\text{CuO} \cdot 2\text{H}_2\text{O}$ ,  $\text{CuCrO}_4$ ,  $\text{CuCr}_2\text{O}_4$  and CuO according to reactions

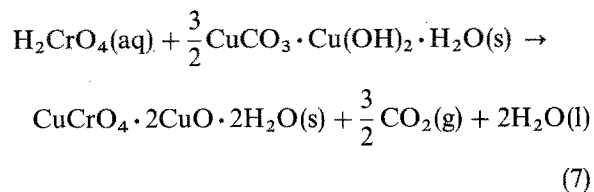


respectively, in oxygen and air obtained in this study, have been compared with the data available in the literature [10–12] for Reactions 4–6.

## 2. Experimental Procedure

### 2.1. Materials

High-purity  $\text{CuCO}_3 \cdot \text{Cu}(\text{OH})_2 \cdot \text{H}_2\text{O}$ ,  $\text{Cr}(\text{VI})\text{O}_3$  and  $\alpha\text{-Al}_2\text{O}_3$  were obtained from Johnson Matthey Ltd (Royston, Hertfordshire, UK).  $\text{CuCrO}_4 \cdot 2\text{CuO} \cdot 2\text{H}_2\text{O}$  was synthesized by precipitating it from aqueous solution of  $\text{Cr}(\text{VI})\text{O}_3$  and  $\text{CuCO}_3 \cdot \text{Cu}(\text{OH})_2 \cdot \text{H}_2\text{O}$  at room temperature (298 K) followed by drying the filtered precipitate in an oven at 373 K in ambient atmosphere. The reaction between aqueous  $\text{Cr}(\text{VI})\text{O}_3$  and  $\text{CuCO}_3 \cdot \text{Cu}(\text{OH})_2 \cdot \text{H}_2\text{O}$  is similar to an acid-base reaction of the type



The formation of  $\text{CuCrO}_4 \cdot 2\text{CuO} \cdot 2\text{H}_2\text{O}$  from components according to Reaction 7 is very rapid and proceeds with a hissing noise due to the evolution of carbon dioxide gas. The compound,  $\text{CuCrO}_4 \cdot 2\text{CuO} \cdot 2\text{H}_2\text{O}$ , was found to be dirty brown in colour.

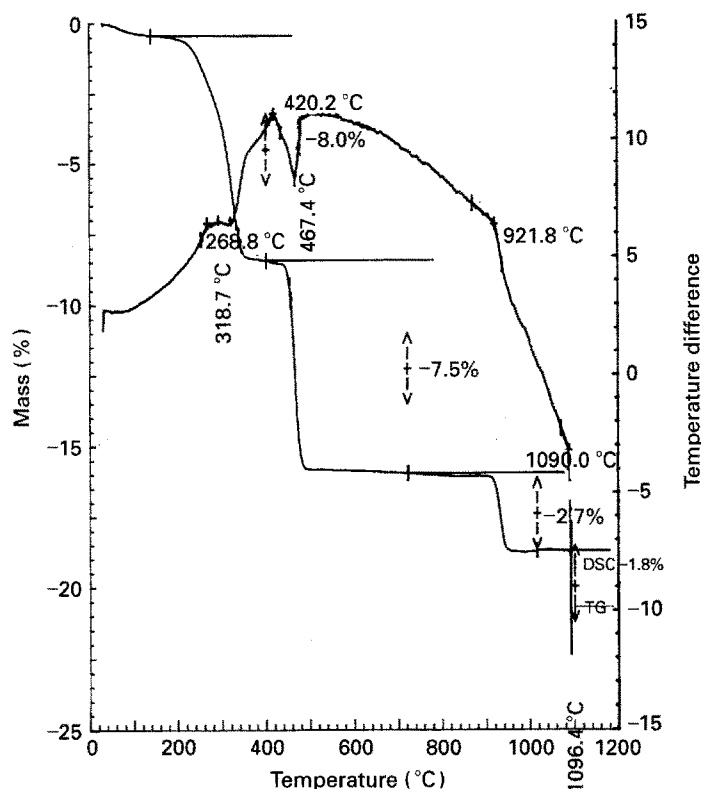
### 2.2. Procedure

The TGA and DSC studies for the compound  $\text{CuCrO}_4 \cdot 2\text{CuO} \cdot 2\text{H}_2\text{O}$  were carried out employing

a NETZSCH STA 409 which was capable of performing TGA and DSC simultaneously. The TGA and DSC experiments were conducted in controlled atmosphere of pure oxygen and air. The initial sample weight was maintained between 33 and 35 mg in all the experiments and the gas flow rate was kept constant at  $50 \text{ cm}^3 \text{ min}^{-1}$ . The heating rate during the TGA and DSC experiments was maintained at  $1 \text{ K min}^{-1}$ . The reference material used for TGA and DSC studies was high-purity calcined  $\alpha\text{-Al}_2\text{O}_3$ .

The formation of various phases at each stage of decomposition was identified by equilibrating  $\text{CuCrO}_4 \cdot 2\text{CuO} \cdot 2\text{H}_2\text{O}$  compound 25 K above the decomposition temperature, obtained by TGA/DSC, for a prolonged period of time until no weight change of the sample was recorded. The decomposition product was then subjected to X-ray diffraction analysis (XRD) using nickel-filtered  $\text{CuK}_\alpha$  radiation in order to identify the phases present.

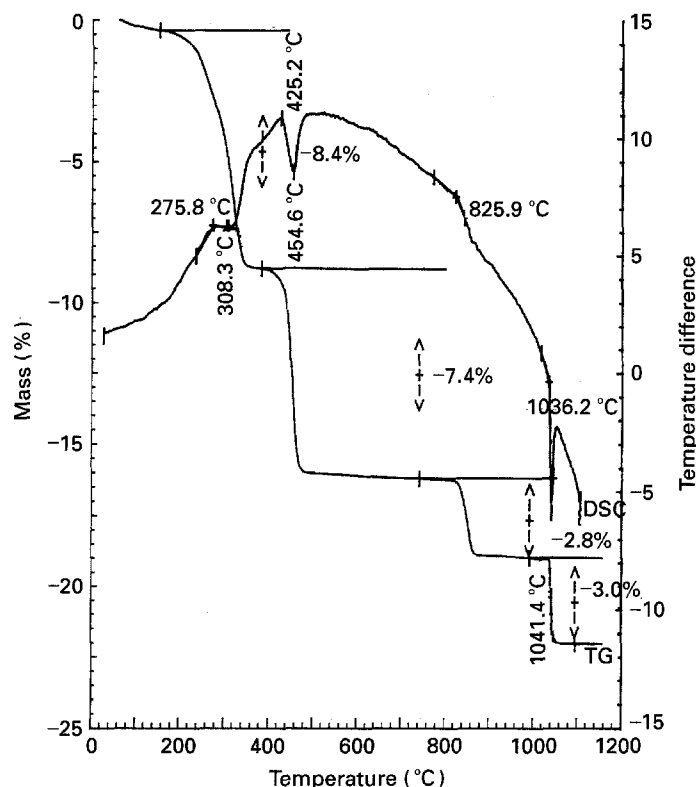
The morphology of  $\text{CuCrO}_4$  and the mixture of  $\text{CuO} + \text{CuCr}_2\text{O}_4$ , Adkin's catalyst, formed as a result of the decomposition of  $\text{CuCrO}_4 \cdot 2\text{CuO} \cdot 2\text{H}_2\text{O}$  at 798 K was studied using the scanning electron microscope (SEM). The sample for SEM studies was prepared by dispersing the material in acetone using an ultrasonic bath and then evaporating a couple of drops placed on the SEM stub. This was followed by coating the material by carbon.



Identity no.	Sample #1	Sample	AN 519/93	34.94 mg TG	50.0 mg	---
Date	31 Mar 1993	Reference	Alumina	32.60 mg DSC	500 uV	---
Operator	B. Mandalia	Atmosphere	Flowing OX/50			
Laboratory	CTC	Crucible	Alumina			

Seg. 1:20 °C/1.00/1150 °C

Figure 1 TGA and DSC profile of  $\text{CuCrO}_4 \cdot 2\text{CuO} \cdot 2\text{H}_2\text{O}$  in a pure oxygen atmosphere.



Identity no. Sample #1 Sample AN 519/93 34.37 mg TG 50.0 mg I-  
 Date 24 Mar 1993 Reference Alumina 32.60 mg DSC 500 uV I-  
 Operator B. Mandalia Atmosphere Flowing Al/60  
 Laboratory CTC Crucible Alumina

Seg. 1: 20 °C/1.00/1150 °C

Figure 2 TGA and DSC trace of  $\text{CuCrO}_4 \cdot 2\text{CuO} \cdot 2\text{H}_2\text{O}$  in air.

TABLE I Comparison of the onset temperature for the decomposition Reactions 3–6 obtained in this investigation with that reported in the literature [10–12]

Reaction no.	Atmosphere	Onset Temperature (K)			
		[10]	[11]	[12]	This investigation
3.	Oxygen				463
	Air				453
4.	Oxygen		735 ± 10		740
	Air		699 ± 10		698
5.	Oxygen	1167 ± 10			1173
	Air	1065 ± 10			1073
6.	Oxygen			1389 ± 10	1388
	Air			1299 ± 10	1299

### 3. Results and discussion

The TGA and DSC profiles  $\text{CuCrO}_4 \cdot 2\text{CuO} \cdot 2\text{H}_2\text{O}$  between 298 and 1373 K in pure oxygen, and air are shown in Figs 1 and 2, respectively. It can be clearly seen from Figs 1 and 2 that in both oxygen and air the initial material,  $\text{CuCrO}_4 \cdot 2\text{CuO} \cdot 2\text{H}_2\text{O}$  decomposes into four different phase assemblages depending on the temperature. However, the temperature range for the coexistence of each phase assemblage decreases as the partial pressure of oxygen is reduced from  $1.01 \times 10^5$  Pa in pure oxygen to  $2.12 \times 10^4$  Pa in air. The phases present after each stage of decomposition were identified by XRD analysis. The change

in phase assemblage characterized by the TGA, DSC and XRD analysis of the sample as a function of increase in temperature occurs according to Reactions 3–6.

The decomposition temperature for the compounds  $\text{CuCrO}_4 \cdot 2\text{CuO} \cdot 2\text{H}_2\text{O}$ ,  $\text{CuCrO}_4$ ,  $\text{CuCr}_2\text{O}_4$  and  $\text{CuO}$ , in pure oxygen and air according to Reactions 3–6 are given in Table I. Earlier, Jacob *et al.* [10–12] determined the Gibbs energy change for Reactions 4–6 by a solid-state galvanic cell technique. The decomposition temperatures corresponding to Reactions 4–6 obtained by extrapolating their data are compared with present results in Table I. It can be clearly seen

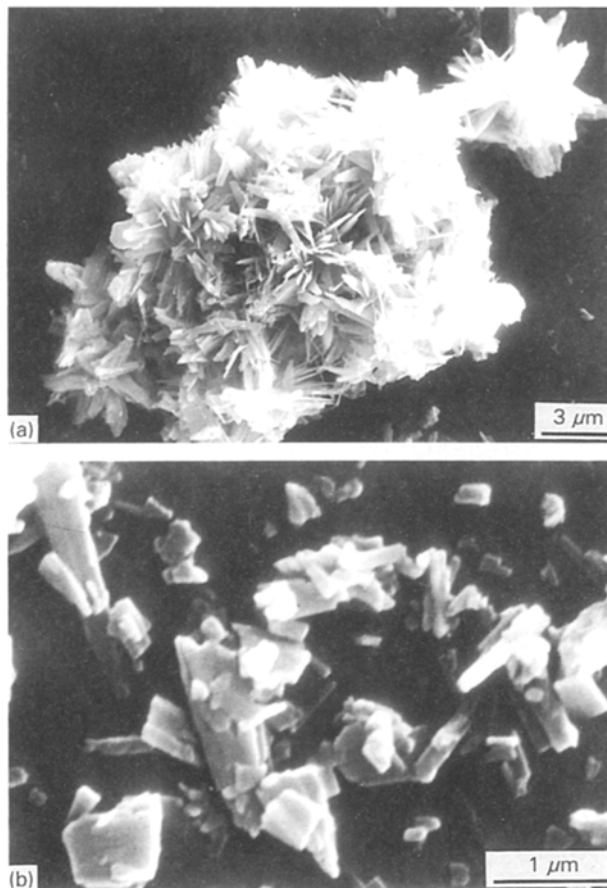


Figure 3 (a, b) Scanning electron micrographs of  $\text{CuCrO}_4 \cdot 2\text{CuO} \cdot 2\text{H}_2\text{O}$  precipitate.

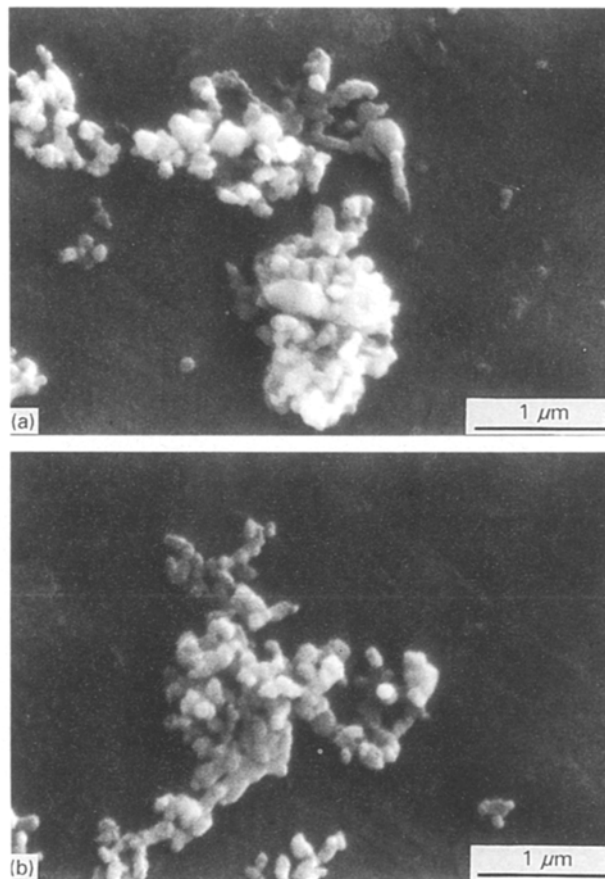


Figure 4 (a, b) Scanning electron micrographs of  $\text{CuCr}_2\text{O}_4 + \text{CuO}$  powder formed after decomposition of  $\text{CuCrO}_4 \cdot 2\text{CuO} \cdot 2\text{H}_2\text{O}$  at 798 K.

that the present results are in excellent agreement with those of Jacob *et al.* [10–12] for Reactions 4–6. The decomposition temperature of the compound  $\text{CuCrO}_4 \cdot 2\text{CuO} \cdot 2\text{H}_2\text{O}$  has been measured for the first time in the present investigation. Based on the TGA results obtained in this study in pure oxygen, shown in Fig. 1, the compounds  $\text{CuCrO}_4$  formed after the first stage of decomposition, and  $\text{CuCr}_2\text{O}_4$  formed as a result of second stage of decomposition, exhibit significant oxygen non-stoichiometry. The DSC results indicate that the enthalpy change for Reactions 3–6 is positive and hence the process is endothermic. This is also in agreement with the value of second-law enthalpy change for Reactions 4–6 obtained by Jacob *et al.* [10–12].

In order to study the morphological features of the starting material,  $\text{CuCrO}_4 \cdot 2\text{CuO} \cdot 2\text{H}_2\text{O}$ , and the Adkin's catalyst,  $\text{CuCr}_2\text{O}_4 + \text{CuO}$ , formed after decomposing  $\text{CuCrO}_4 \cdot 2\text{CuO} \cdot 2\text{H}_2\text{O}$ , both the materials were observed under the SEM. The examination of powders of  $\text{CuCrO}_4 \cdot 2\text{CuO} \cdot 2\text{H}_2\text{O}$  under the SEM revealed that the crystals had a rectangular plate-like structure, as shown in Fig. 3. The length of the platelets was less than 1–1.5  $\mu\text{m}$ , and the width was approximately less than 0.5  $\mu\text{m}$ . This material was then decomposed at 798 K to give Adkin's catalyst consisting of a mixture of  $\text{CuCr}_2\text{O}_4 + \text{CuO}$ . Fig. 4 shows the fine, uniform particles of the mixture of  $\text{CuCr}_2\text{O}_4 + \text{CuO}$  as seen under the SEM. The particle

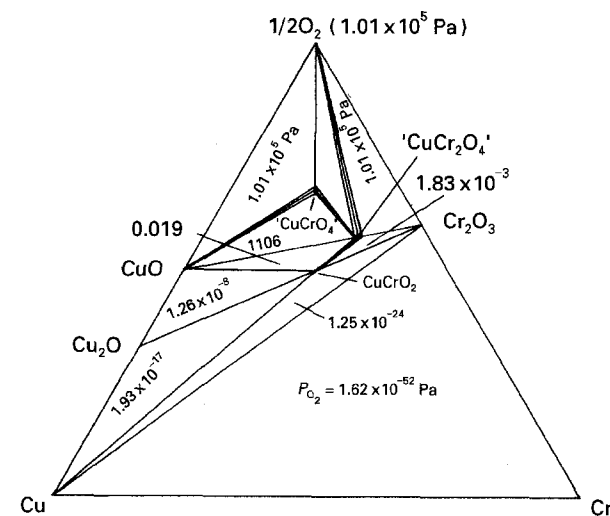


Figure 5 The isothermal section of the Cu–Cr–O phase diagram at 600 K.

size of this material is probably less than 0.1  $\mu\text{m}$  having a uniform spherical geometry.

Based on the results obtained in this study and the earlier results reported by Jacob *et al.* [10–12], the ternary phase diagram of Cu–Cr–O at 600 and 1150 K has been composed as shown in Figs 5 and 6, respectively. The approximate non-stoichiometry of  $\text{CuCrO}_4$  and  $\text{CuCr}_2\text{O}_4$  are indicated on the phase diagrams.

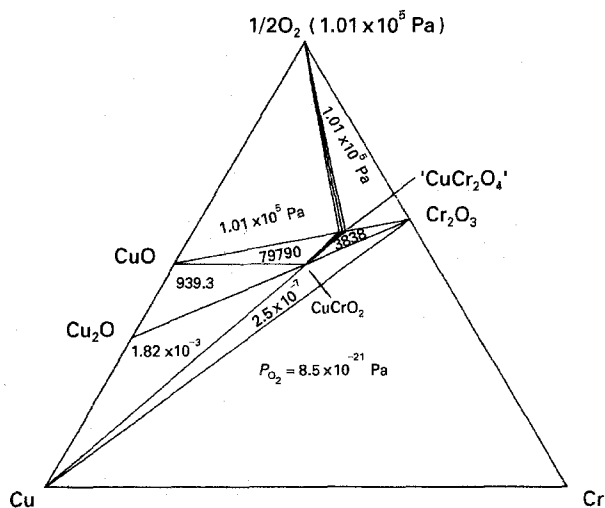


Figure 6 The ternary phase diagram of Cu-Cr-O at 1150 K.

### Acknowledgements

The author thanks Baresh Mandalia, Cookson Technology Centre, for the TGA/DSC of the material, the European Economic Communities (EEC) for financial support, and Miss J. Priestley for her assistance in preparing the manuscript.

### References

1. H. ADKINS and H. CONNOR, *J. Am. Chem. Soc.* **53** (1931) 1091.
2. H. ADKINS, E. E. BURGOYNE and H. J. SCHNEIDER, *ibid.* **72** (1950) 2626.
3. J. D. STROUPE, *ibid.* **71** (1949) 569.
4. A. HIMURA, Y. INOUE and I. YASUMORI, *Bull. Chem. Soc. Jpn* **56** (1983) 2203.
5. M. STAMMLER and M. PYZYNA, *Adv. X-ray Anal.* **7** (1964) 229.
6. L. WALTER-LEVY and M. GOREAUD, *Bull. Soc. Chim. Fr.* **3** 1 (1973) 830.
7. B. G. ERENBURG, V. P. FATEYEVA, A. I. MINKOV, L. M. SHADRINA and E. S. STOYANOV, *Izv. Sib. Otd. Akad. Nauk SSSR Ser. Khim. Nauk* (4) **2** (1981) 54.
8. M. S. KOSNYREVA, A. I. PURTOV, I. I. KALINITCHENKO and D. M. DOROFYEVA, *Ah. Prikl. Khim. (Leningrad)* **46** (1976) 2515.
9. F. HANIC, L. HORVATH, G. PLESCH and L. GALIKOVA, *J. Solid State Chem.* **59** (1985) 190.
10. K. T. JACOB, G. M. KALE and G. N. K. IYENGAR, *J. Mater. Sci.* **21** (1986) 2753.
11. K. T. JACOB, G. M. KALE and Y. WASEDA, *Thermochim. Acta* **208** (1992) 341.
12. K. T. JACOB, and C. B. ALCOCK, *J. Am. Ceram. Soc.* **8** (1975) 192.

Received 29 July  
and accepted 11 August 1994